THE JOURNAL OF PHYSICAL CHEMISTRY B

Article

pubs.acs.org/JPCB

Exploration of pH-Dependent Behavior of the Anion Receptor Pocket of Subdomain IIA of HSA: Determination of Effective Pocket Charge Using the Debye–Hückel Limiting Law

Priyanka Bolel, Shubhashis Datta, Niharendu Mahapatra, and Mintu Halder*

Department of Chemistry, Indian Institute of Technology Kharagpur, Kharagpur-721302, India

Supporting Information

ABSTRACT: Protein–ligand electrostatic interaction can be looked upon as ion receptor–ligand interaction, and the binding cavity of protein can be either an anion or cation receptor depending on the charge of the guest. Here we focus on the exploration of pH-modulated binding of a number of anionic ligands, specific to the subdomain IIA cavity of HSA, such as carmoisine, tartrazine, cochineal red, and warfarin. The logarithm of the binding constant is found to vary linearly with the square-root of ionic strength, indicating applicability of the Debye–Hückel limiting law to protein–ligand electrostatic binding equilibrium, and concludes that the subdomain IIA cavity is an anion receptor. The present approach is very unique that one can calculate the effective charge of the protein-based anion receptor pocket, and the calculated charge has been found to vary between +1 and +3 depending on the pH and ligand itself. The study also indicates that in such cases of specific ligand binding the pocket charge rather than the overall or surface charge of the macromolecule seems to have a paramount role in determining the strength of interaction. For the first time, it is demonstrated that the Debye–Hückel interionic interaction model can be successfully applied to understand the protein-based receptor–ligand electrostatic interaction in general.

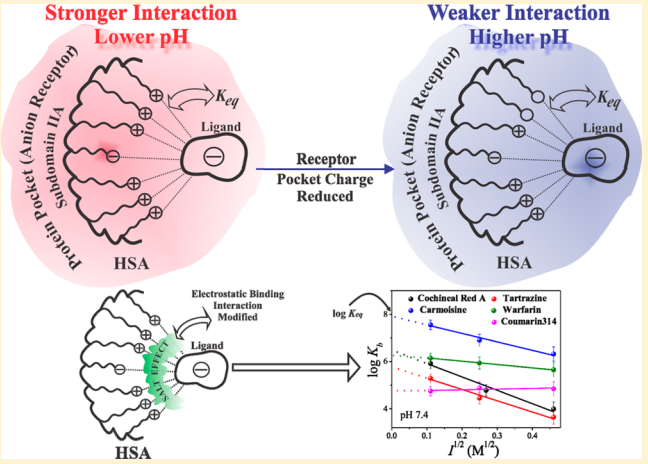

1. INTRODUCTION

In recent years, studies on the receptor–ligand interactions have been found to be of immense importance in the material and biological systems for both basic science and applicative reasons.[1−4] Receptor–ligand interaction is widely used in different biochemical and biological processes such as enzyme–substrate recognition, molecular recognition, hormone action, signal transduction, and cell communications.[5−9] In such cases, different types of weak interactions are operative, e.g., H-bonding, π-stacking, hydrophobic effects, and so on.[10−16]

Apart from these, electrostatic interaction is another very significant factor in receptor–ligand systems. For example, poly amino molecules, that are protonated in aqueous media around the physiological pH, have been widely used for their ability to interact strongly with the negatively charged phosphate groups of nucleotides.[17] Importantly, electrostatic interactions are also known to play primary roles in many protein–ligand associations and rates of protein–ligand interaction.[18,19]

Since the pioneering work of Linderstrøm-Lang,[20] significant progress has been made in the qualitative and quantitative aspects of electrostatic interactions. A variety of computational methods and algorithms for studying proteins and their interactions with other molecules have been constructed in molecular dynamics simulations[21] and a molecular docking approach[22] to predict and analyze protein functions, such as catalytic activity, folding pathway, stability, solubility, and ligand/drug binding specificity.[23,24]

Numerous studies have demonstrated the functioning of electrostatic interactions between the basic side chain of amino acid residues of proteins and the charge-carrying groups of the ligand partner.[25,26] Because of the charge complementarities, one may expect that electrostatic interactions favor formation of protein–ligand complexes (ion pairs). Such expectations are confirmed experimentally, among others, by an approach using site-directed mutagenesis[27] to modify charge at a particular site on the protein surface, originated by Fersht et al.[28] Kinetic and equilibrium measurements with mutation in the barnase–barstar interface confirmed that neutralization of charge-carrying residues significantly reduces the binding constant.[29] Moreover, the strength of electrostatic interaction is in general known to decrease as the salt concentration increases, because ion-pair formation between protein and ligand becomes less favorable in the solution having a high concentration of salt.[30−32]

Received: July 16, 2013
Revised: December 6, 2013
Published: December 10, 2013

dx.doi.org/10.1021/jp407057f | J. Phys. Chem. B 2014, 118, 26–36

The success of the approach for predicting physical and biochemical characteristics of these systems will only be possible if we are able to evaluate electrostatic forces and energies in and around the protein. Such calculations in biomolecules arguably present one of the largest obstacles, since electrostatic phenomena in these systems are quite complex and many studies are needed to understand the factors that may be crucial there.

Although the quantitative evaluation of electrostatic interaction between protein−DNA,[33] protein−RNA,[34] DNA−metal complex,[35] and ligand−nucleic acid complex[36] has been made quite frequently using the Poisson−Boltzmann (PB) model, polyelectrolyte theory, the similar studies dealing with protein−ligand/dye interaction are very rare. Moreover, literature reports indicate that the primary focus of protein−ligand/dye binding studies is simply the determination of binding mode and identification of possible binding site(s) in protein.[37] In this regard, HSA is one of the extensively studied systems. This is often considered as a versatile carrier protein in humans, and its most important physiological role is to solubilize different types of molecules/drugs in blood plasma and regulate their delivery to the target *in vivo* and *in vitro*. In recent works, we have shown that ligands with negatively charged sulfonate groups such as cochineal red A, tartrazine, and carmoisine bind specifically in subdomain IIA of HSA by electrostatic interaction. Different positively charged amino acid side chains available in subdomain IIA are responsible for the interaction.[38−40] Therefore, such a protein pocket can be a good mimic of receptor ligand systems, in general. When receptor−ligand interaction is guided by electrostatic forces, the receptor can be classified as an anion or cation receptor depending on the charge on the ligand.[41] The advantage of this protein-based receptor is that the different ionizable amino acid side chains present within the pocket may undergo charge alterations induced by pH[42] and thus the strength of receptor−ligand interaction can be modulated. Very recently, some quantitative approach has also been reported by us with the serum albumin−tartrazine case, which addresses how the electrostatic interaction between the anionic ligand and protein is affected by the change of ionic strength.[38] In that study, we have shown the applicability of the Debye−Hückel theory[43,44] in explaining the modulation of binding thermodynamics in the presence of salt.

On the basis of the general understanding of Debye−Hückel theory of interionic interaction, the presence of an inert electrolyte (salt, e.g., NaCl) will tend to alter the activity coefficient of the ionic species in solution involved in binding equilibrium and this may result in either an increase or decrease of the binding constant. Upon replacing the activity coefficient of ionic species in the equilibrium constant with corresponding Debye−Hückel limiting law expressions (for dilute solutions), one can express the binding constant as a function of ionic strength of the medium (provided only inert salt is varied). The final expression for the equilibrium constant contains terms that represent charge on the interacting partners. Now the charge in the protein pocket (some specific pocket) can be determined assuming the pocket charge to be a point charge, provided the ligand charge is known.

Affinity of drugs to plasma proteins is an important pharmacological parameter, since it frequently affects the distribution and elimination of drugs as well as the duration and intensity of its physiological action.[45,46] Drugs are subjected to the influences of many factors *in vivo* including dietary habits.[47] Some food contains synthetic colorants; therefore, their competition with drugs for binding with the protein may occur. The relative strengths of these binding processes are important, since the competition between the drug and ligand (food colorant/dye) can interfere with the transport function of serum albumins to such an extent that certain drugs initially bound by HSA may also be released if the protein binds the food colorant stronger. The pharmacological effect is closely related to the free concentration of drug at its site of action.[48] Hence, the competition will affect the concentration of free drugs in the plasma, leading to higher activity or toxicity.[49] Thus, the exploration of HSA−food dye/ligand binding can be very important in pharmacology.

In the present study, we have explored the interaction between a fixed receptor pocket in subdomain IIA of HSA and a number of ligands (shown in Scheme 1) differing in the total charge, specific to the same pocket, e.g., cochineal red A (CR, charge = −3), tartrazine (TZ, charge = −3), carmoisine (CM, charge = −2), Na-warfarin (WF, charge = −1), and a neutral ligand coumarin 314 (C314, charge = 0) fluorimetrically.

Scheme 1. Molecular Structure of (a) Cochineal Red A (CR), (b) Tartrazine (TZ), (c) Carmoisine (CM), (d) Coumarin 314 (C314), and (e) Na-Warfarin (WF) and (f) Crystal Structure of HSA (PDB ID: 1AO6)

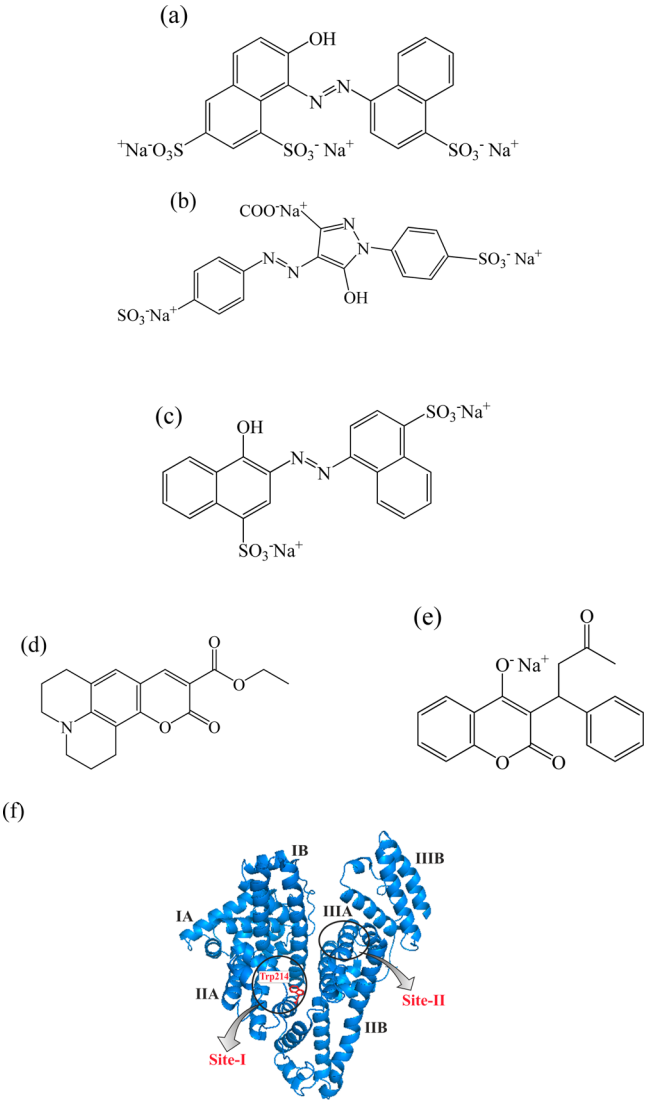

dx.doi.org/10.1021/jp407057f | J. Phys. Chem. B 2014, 118, 26−36

The studied ligands (CR, TZ, and CM) are well-known synthetic azo food colors that are found in common food products such as beverages, dry mix products, candies, dairy products, sugar confectioneries, and bakery products.[50] Coumarins constitute a very large family of compounds and exhibit interesting fluorescence properties, which include a high degree of sensitivity to their local environment, including polarity and viscosity.[51] Warfarin is an anticoagulant normally used in the prevention of thrombosis and thromboembolism, the formation of blood clots in the blood vessels and their migration elsewhere in the body.[52]

In our study, pH and ionic strengths are varied purposely to find out their effect on the binding constant. It may be noted that serum albumins have different pH-dependent conformational isomers, but the normal form (N)[53] of HSA has been chosen for our experiment by selection of the pH range 4.8−7.3. It is also verified from the little change in helical content that the secondary structure of HSA is not significantly affected within the experimental pH window (discussed later with CD data in section 3.1). Between pH 4.8 and 7.3, CR and TZ are tri-negative ($pK_{a,CR}$ = 11.24, $pK_{a,TZ}$ = 9.40)[54] and CM is di-negative ($pK_{a,CM}$ = 7.9).[39] C314 is a carboxylic ester which is found to be somewhat unstable at pH 4.8 probably due to hydrolysis, and this has been indicated by the change in absorbance with time (data not shown), but at the other studied pH, the probe has been found to be stable. Therefore, to be on the safer side, the lowest studied pH for C314 is kept at 5.6. Also in the case of WF, the lowest studied pH has been kept at 5.6 to avoid possible complications arising out of different forms owing to its pK_a of 4.9.[55] The ionic strength of the system is varied by varying the added NaCl concentration from 0 to 0.2 M. Experimental results are further substantiated with molecular docking simulations and crystal structure analysis of the known HSA−warfarin complex.[56]

To the best of our knowledge, the present study is an attempt to demonstrate the applicability of the Debye−Hückel interionic interaction model to understand the general behavior of the ion-receptor pocket in subdomain IIA of HSA. This novel approach also entails us to know whether the effective charge of the receptor pocket is the same for any anionic ligand or it may change depending on the ligand itself or its charge.

2. MATERIALS AND METHODS

2.1. Materials. HSA (~99%, essentially fatty acid free) is purchased from Fluka. All dyes are purchased from Sigma-Aldrich, USA. Warfarin is purchased from TCI-Japan. For preparing solutions of various ionic strengths, the required weighed amount of NaCl (analytical grade, Merck) is added to 5 mM sodium phosphate buffer, and this NaCl-containing buffer is used to make various protein:ligand compositions in salt variation studies. Ultrapure water is used throughout the study. All solutions are prepared in 5 mM phosphate buffer of different pH, i.e., 4.8, 5.6, 6.4, and 7.3. The pH of solutions is measured with a precalibrated EUTECH pH 510 ion pH-meter.

2.2. UV−vis Absorbance Spectra. UV−vis absorbance spectra are recorded on a Shimadzu UV-2450 absorption spectrophotometer against a solvent blank reference in the wavelength range 300−650 nm.

2.3. Fluorescence Measurements. All corrected steady-state fluorescence spectra are recorded in a 1 cm path length quartz cuvette at 298 K using a Jobin Yvon-Spex Fluorolog-3 spectrofluorimeter equipped with a thermostatic cell holder. Quenching experiments are performed by keeping the concentrations of HSA fixed at 2 μM. An excitation wavelength of 295 nm (slit width = 10 nm/3 nm) is used in all cases for selective excitation of the tryptophan (Trp) residue, and emission spectra are recorded from 310 to 470 nm.

The fluorescence ratio F_0/F is calculated, where the numerator corresponds to fluorescence intensity in the absence and the denominator is the corresponding value in the presence of quencher (ligand). This fluorescence ratio has been corrected for the absorption of quencher at the excitation and emission wavelengths of the fluorophore using the procedure described elsewhere[57] (see the Supporting Information for details).

The corrected fluorescence ratios are used in calculating the binding constant (K_b) employing eq 1[58] as follows, where "n" is the number of binding sites and [Q] is the quencher concentration.

$$\log\left(\frac{F_0 - F}{F}\right) = \log K_b + n\log[Q] \quad (1)$$

In the case of the HSA−Na−warfarin binding study, we have followed the literature reported method[59] to calculate the affinity.

2.4. Circular Dichroism Spectra. Circular dichroism (CD) spectra are recorded on a Jasco-810 automatic recording spectropolarimeter at 298 K under constant nitrogen flush over a wavelength range of 190−260 nm with a scan speed of 50 nm/min. A quartz cell of 0.1 cm path length is use, and each spectrum is the average of three successive scans. A corresponding buffer solution running under the same condition is taken as the blank and subtracted from the experimental spectra. The CD spectra of HSA are recorded at all experimental pH values and also in the presence of 0.05 and 0.2 M added NaCl concentration. Here the concentration of protein is kept at 8 μM.

2.5. Molecular Docking Study. The 3D structure of HSA (PDB ID: 1AO6) is used for molecular docking simulations. The structure of the ligand is optimized by PM3 prescription using MOPAC 2002.[60] Later, the ligand is docked into the 3D structure of HSA by AutoDock 4.2.[61] AutoDock 4.2 uses the Lamarckian genetic algorithm to search for the optimum binding site of small molecules in the protein. To recognize the binding sites in HSA, docking is done; the grid sizes are set to 60, 60, and 60 along the X-, Y-, and Z-axes with a 0.5 Å grid spacing. The centers of the grid are set to 24.366, 34.571, and 33.095 Å corresponding to Trp214. The Auto Docking parameters used are as follows: GA population size, 150; maximum number of energy evaluations, 250 000. A maximum of 50 conformers is considered for each ligand, and the RMS (root-mean-square) cluster tolerance has been set to 2.0 Å. The accessible surface area (ASA) of uncomplexed protein and their docked complex with ligands are calculated using Discovery Studio Visualizer 2.5 software of Accelrys Software Inc.[62] The change in ASA for a residue is given by $\Delta ASA = ASA_{protein} - ASA_{protein-ligand}$.

2.6. Data Analysis. All data are represented as mean ± SD. Experiments are performed in triplicates. All graphical representations and statistical analyses are done using Origin.

3. RESULTS AND DISCUSSION

3.1. Circular Dichroism Spectra. The α-helix content of HSA has been calculated in the presence of different added salt concentrations within the pH range 4.8−7.3, and they are tabulated in Table 1. The results show that the helical content

dx.doi.org/10.1021/jp407057f | J. Phys. Chem. B 2014, 118, 26−36

Table 1. α-Helix Content (%) of HSA at Different pH and Salt Concentrations at 298 K

	α-helix content (%)		
pH	0.0 M NaCl	0.05 M NaCl	0.2 M NaCl
4.8	56.3 ± 0.1	57.4 ± 0.1	58.2 ± 0.1
5.6	56.9 ± 0.1	57.7 ± 0.1	58.5 ± 0.1
6.4	57.6 ± 0.1	58.2 ± 0.1	59.1 ± 0.1
7.3	58.1 ± 0.1	58.9 ± 0.1	59.9 ± 0.1

is not affected significantly due to variation of pH or added salt concentration. Thus, the added electrolyte and pH do not seem to have a considerable effect on the secondary structure of HSA.

3.2. Fluorescence Studies: Expression of Binding Constant Using the Debye–Hückel Limiting Law. We have monitored quenching of the intrinsic tryptophan fluorescence of HSA by several site-I (subdomain IIA) specific ligands (CR, TZ, CM, C314, and WF). The site-I specificity of these ligands has been confirmed from competitive binding[38,39] (results of competitive binding for C314 are shown in the Supporting Information, Figure S1) and crystal structure data of the WF–HSA complex.[56] Except for C314, all the ligands bind primarily by electrostatic forces, which is evident from thermodynamic data and salt effects (see Figures S2, S3, and S4 in the Supporting Information) and also from reports elsewhere.[38,39] To make sure that ionic interactions are not significantly perturbed, we have carried out the entire quenching and other spectroscopic experiments in dilute phosphate buffer (5 mM) of appropriate pH. Only for ionic strength variation studies, we have used buffer solution containing the required amount of added NaCl.

Figure 1 displays the fluorescence quenching plots of HSA by CR, TZ, CM, and C314 at pH 7.3, and the inset shows

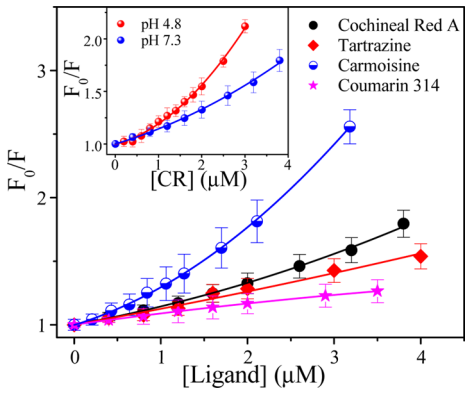

Figure 1. Plot of fluorescence quenching of HSA by cochineal red A, tartrazine, carmoisine, and coumarin 314 at pH 7.3 and 298 K. The inset shows the quenching plot for the HSA–cochineal red A system at pH 4.8 and 7.3. Symbols with cap include error bar.

quenching by CR at two different pH. The respective calculated binding constants are presented in Table 2. Here the binding affinity has been found to reduce with increase of pH from 4.8 to 7.3 for both CR and TZ. For WF, the binding constant also decreased by about 46% when switching from pH 5.6 to 7.3. For C314, we have not seen any perceptible change of the binding constant with pH. Also, for CM, the pH dependence of the binding constant has not been observed.

The stoichiometry of the complex between HSA and CR/TZ/CM is determined to be 1:1,[38,39] using the modified Job's method of continuous variation.[63,64] We have also determined the stoichiometry for the HSA–C314 complex which is found to be 1:1 too (see Figure S5 in the Supporting Information). Warfarin is known to form a 1:1 complex with HSA.[65] Now let us consider the following scheme (Scheme 2) of binding of ligand (D) with the receptor pocket of protein (P) in a simple 1:1 stoichiometry (as is experimentally observed) producing complex (PD). Here, Z_P and Z_D are the charges (sign inclusive) in the protein pocket (receptor pocket) and ligand, respectively. In this case, either both of them or one may be charge-carrying or both of them can be neutral. The binding equilibrium can be considered as shown in Scheme 2.

Scheme 2. Binding Equilibrium (A) for 1:1 Complex Formation between Ligand and Protein, and the Expression (B) for the True Thermodynamic Binding Constant (K_{eq})

$$P^{Z_P} + D^{Z_D} \rightleftharpoons PD^{Z_P+Z_D} \quad \text{.....(A)}$$

$$K_{eq} = \frac{a_{PD}}{a_P a_D} = \frac{c_{PD}}{c_P c_D} \times \frac{\gamma_{PD}}{\gamma_P \gamma_D} = K_b \times \frac{\gamma_{PD}}{\gamma_P \gamma_D} \quad \text{.....(B)}$$

In Scheme 2, K_{eq} is the true thermodynamic binding constant, a is the activity of the respective species, γ is the corresponding activity coefficient, and K_b is the observed binding constant. I is the ionic strength[66] of the medium. Since the activity depends on the concentration of the reactant and the ionic strength of the medium, the observed binding constant will depend on the ionic strength and charge of the species taking part in the interaction, provided it is predominantly electrostatic in origin. Thus, for dilute solutions, applying the Debye–Hückel limiting law.[43,44]

$$\begin{aligned}\log K_{eq} &= \log K_b + [\log \gamma_{PD} - \log \gamma_P - \log \gamma_D] \\ &= \log K_b - [A(Z_{PD}{}^2 - Z_P{}^2 - Z_D{}^2)]I^{1/2} \\ &= \log K_b - [A\{(Z_P + Z_D)^2 - Z_P{}^2 - Z_D{}^2\}]I^{1/2} \\ &= \log K_b - 2{\cdot}A{\cdot}(Z_P{\cdot}Z_D)I^{1/2}\end{aligned}$$

For water at 298 K and $A = 0.509$,

$$\log K_b = \log K_{eq} + 1.018{\cdot}Z_P{\cdot}Z_D I^{1/2} \quad (2)$$

Now Z_P should be the effective local charge of the receptor pocket. The plot of log K_b vs $I^{1/2}$ will be a straight line with positive, negative, or zero slope depending on the sign of the product ($Z_P{\cdot}Z_D$), and the intercept is log K_{eq}. The positive slope means the interaction is either (+·+) or (−·−) type, negative slope corresponds to (+·−) or (−·+) interaction, whereas zero slope means (0·0) or (±·0) type interaction; the last option is effectively a non-electrostatic case. If the charge on the exogenous ligand is known, we can find out Z_P. To our utter surprise, we have observed that the results corroborate nicely with charge type as predicted by eq 2.

A linear dependency with *negative* slope in the plots of log K_b vs $I^{1/2}$ (Figure 2) is found for all three negatively charged ligands (CR, TZ, CM) and WF, whereas for the neutral C314 no change in the slope of the plot is found. Thus, it may be concluded that the negatively charged ligands bind to the net positively charged binding pocket (site-I) of HSA and this

dx.doi.org/10.1021/jp407057f | J. Phys. Chem. B 2014, 118, 26–36

Table 2. Binding Constants (K_b), Number of Binding Sites (n), Thermodynamic Binding Constants (K_{eq}), and Product of Protein−Ligand Charges ($Z_D \cdot Z_P$) for HSA−Different Ligand Systems with NaCl Concentration in 5 mM Phosphate Buffer of pH[a] 4.8, 5.6, 6.4, and 7.3 at 298 K

	pH 4.8			pH 5.6			pH 6.4			pH 7.3		
(M)	K_b[b]	n	K_{eq} ($Z_D \cdot Z_P$)	K_b[b]	n	K_{eq} ($Z_D \cdot Z_P$)	K_b[b]	n	K_{eq} ($Z_D \cdot Z_P$)	K_b[b]	n	K_{eq} ($Z_D \cdot Z_P$)
						CR						
0	$(4.8\pm0.2)\times10^8$	1.5 ± 0.04	$(1.7 \pm 0.1) \times 10^9$ (−7.7 ± 0.03)	$(3.1 \pm 0.2) \times 10^8$	1.4 ± 0.1	$(7.7 \pm 0.3) \times 10^8$ (−7.8 ± 0.5)	$(2.5 \pm 0.3) \times 10^6$	1.2 ± 0.1	$(7.2 \pm 0.3) \times 10^6$ (−5.3 ± 0.3)	$(8.3 \pm 0.3) \times 10^5$	1.1 ± 0.1	$(2.7 \pm 0.3) \times 10^6$ (−5.4 ± 0.3)
0.06	$(1.6\pm0.1)\times10^7$	1.3 ± 0.04		$(3.0 \pm 0.12) \times 10^6$	1.2 ± 0.1		$(3.2 \pm 0.4) \times 10^5$	1.1 ± 0.1		$(6.0 \pm 0.2) \times 10^4$	1.0 ± 0.1	
0.2	$(5.1\pm0.2)\times10^5$	1.1 ± 0.1		$(2.9 \pm 0.11) \times 10^5$	1.1 ± 0.1		$(2.5 \pm 0.4) \times 10^4$	1.0 ± 0.1		$(9.8 \pm 0.5) \times 10^3$	0.9 ± 0.2	
						TZ						
0	$(3.3\pm0.1)\times10^7$	1.3 ± 0.05	$(1.9 \pm 0.4) \times 10^8$ (−9.60 ± 0.4)	$(1.8 \pm 0.1) \times 10^7$	1.3 ± 0.1	$(5.6 \pm 0.1) \times 10^7$ (−8.4 ± 0.4)	$(1.2 \pm 0.2) \times 10^5$	0.9 ± 0.1	$(2.6 \pm 0.4) \times 10^5$ (−4.6 ± 0.3)	$(1.96 \pm 0.2) \times 10^5$	1.0 ± 0.1	$(5.4 \pm 0.3) \times 10^5$ (−4.6 ± 0.2)
0.05	$(1.3\pm0.2)\times10^6$	1.2 ± 0.04		$(3.2 \pm 0.2) \times 10^5$	1.1 ± 0.1		$(1.8 \pm 0.2) \times 10^4$	0.9 ± 0.1		$(2.9 \pm 0.3) \times 10^4$	1.0 ± 0.1	
0.2	$(6.4\pm0.5)\times10^3$	0.9 ± 0.1		$(9.6 \pm 0.6) \times 10^3$	0.9 ± 0.1		$(2.1 \pm 0.4) \times 10^3$	0.8 ± 0.2		$(4.4 \pm 0.3) \times 10^3$	1.0 ± 0.1	
						CM						
0	$(3.2\pm0.1)\times10^7$	1.3 ± 0.06	$(6.7 \pm 0.3) \times 10^7$ (−3.3 ± 0.2)	$(3.9 \pm 0.2) \times 10^7$	1.4 ± 0.07	$(8.1 \pm 0.5) \times 10^7$ (−3.9±0.16)	$(3.5 \pm 0.12) \times 10^7$	1.3 ± 0.05	$(9.8 \pm 0.5) \times 10^7$ (−3.4±0.17)	$(3.6 \pm 0.2) \times 10^7$	1.3 ± 0.06	$(7.5 \pm 0.2) \times 10^7$ (−3.4 ± 0.2)
0.05	$(1.6\pm0.2)\times10^7$	1.3 ± 0.06		$(9.5 \pm 0.5) \times 10^6$	1.2 ± 0.1		$(2.9 \pm 0.14) \times 10^7$	1.3 ± 0.06		$(8.1 \pm 0.4) \times 10^6$	1.2 ± 0.06	
0.2	$(1.8\pm0.4)\times10^6$	1.2 ± 0.05		$(1.2 \pm 0.4) \times 10^6$	1.1 ± 0.06		$(2.0 \pm 0.12) \times 10^6$	1.2 ± 0.05		$(2.1 \pm 0.4) \times 10^6$	1.2 ± 0.05	
						WF						
0	NA[c]	NA[c]	NA[c]	$(2.6 \pm 0.2) \times 10^6$	0.8 ± 0.1	$(3.1 \pm 0.2) \times 10^6$ (−2.1 ± 0.2)	$(1.0 \pm 0.1) \times 10^6$	0.8 ± 0.1	$(1.2 \pm 0.1) \times 10^6$ (−1.1 ± 0.1)	$(1.4 \pm 0.1) \times 10^6$	1.0 ± 0.1	$(1.9 \pm 0.2) \times 10^6$ (−1.4 ± 0.1)
0.05	NA[c]	NA[c]	NA[c]	$(7.3 \pm 0.5) \times 10^5$	0.8 ± 0.1		$(6.0 \pm 0.3) \times 10^5$	0.8 ± 0.1		$(8.6 \pm 0.4) \times 10^5$	0.7 ± 0.1	
0.2	NA[c]	NA[c]	NA[c]	$(3.9 \pm 0.6) \times 10^5$	0.6 ± 0.1		$(3.8\pm0.2)\times10^5$	0.6 ± 0.1		$(4.5 \pm 0.3) \times 10^5$	0.5 ± 0.1	
						C314						
0	NA[c]	NA[c]	NA[c]	$(5.8 \pm 0.2) \times 10^4$	0.99 ± 0.03	$(4.6 \pm 0.2) \times 10^4$ (0.20 ± 0.06)	$(3.9 \pm 0.2) \times 10^4$	0.97 ± 0.1	$(4.4 \pm 0.3) \times 10^4$ (0.32 ± 0.1)	$(5.6 \pm 0.2) \times 10^4$	0.97 ± 0.02	$(5.8 \pm 0.2) \times 10^4$ (0.22 ± 0.1)
0.05	NA[c]	NA[c]	NA[c]	$(3.7 \pm 0.3) \times 10^4$	0.95 ± 0.07		$(6.8 \pm 0.3) \times 10^4$	1.0 ± 0.04		$(7.6 \pm 0.3) \times 10^4$	1.0 ± 0.03	
0.2	NA[c]	NA[c]	NA[c]	$(6.6 \pm 0.3) \times 10^4$	0.99 ± 0.03		$(5.5 \pm 0.2) \times 10^4$	1.0 ± 0.1		$(7.0 \pm 0.3) \times 10^4$	0.98 ± 0.03	

[a]The error in pH measurement: ±0.1 unit. [b]Concentrations of protein and ligands are expressed in mol L^{-1}. [c]NA = not attempted.

dx.doi.org/10.1021/jp407057f | J. Phys. Chem. B 2014, 118, 26−36

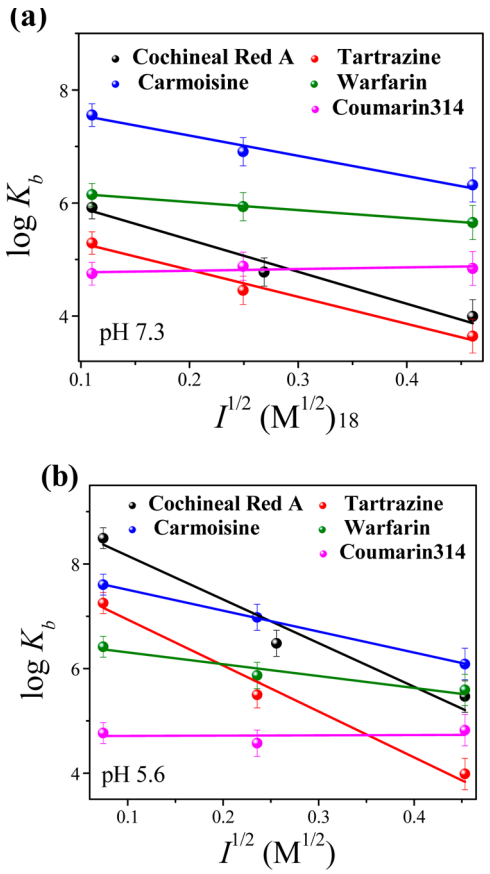

Figure 2. Plot of log K_b vs $I^{1/2}$ for HSA–ligand systems (ligand = cochineal red A, tartrazine, carmoisine, Na-warfarin, and coumarin 314) in 5 mM phosphate buffer at 298 K for (a) pH 7.3 and (b) pH 5.6. Symbols with cap include error bar.

pocket can be regarded as an anion receptor. Since there is no significant structural change due to ionic strength or pH change, as evident from CD data, the observed trend should be due to modulation of the strength of interaction induced by salt.

When the interaction between ligand and protein is primarily electrostatic, the local charge of the binding pocket should be more important than the overall charge of the protein because the binding is confined in a specific location (receptor pocket) and consequently point charge approximation works well.[38] TZ, CR, and WF are found to have weaker interaction with increase of pH; on the other hand, CM and C314 do not have any pH effect. Since the overall charge of HSA at pH 4.8 (pI[67]) is zero, eq 2 predicts no salt effect, and at pH 7.3, some salt effect on binding is expected. However, opposite to these predictions, we have observed a very pronounced salt effect at pH 4.8 (see Figures S2 and S3 in the Supporting Information). Also, it is important to mention that if the overall charge of HSA is rather more important than the pocket charge then the change of pH should have resulted in a similar effect on the binding behavior of all the negatively charged ligands (TZ, CM, and CR) with HSA because pH affects the surface charge more.[42] As mentioned earlier, all the studied ligands bind in the same site of HSA, but importantly, the effect of pH on the binding of CM with HSA is totally different (pH-insensitive) from the other two ligands (TZ and CR). This indicates that the local charge at the ligand binding site (receptor pocket) is more important than the overall charge or surface charge of HSA. Similar application of the Debye–Hückel limiting law has been found to explain the electrostatic effects in the folding of a single domain protein FynSH3,[68] and our very recent report on the effect of salt on the thermodynamics of electrostatic binding of tartrazine with serum albumins has also pointed out a similar conclusion on the importance of the local charge of the binding site.[38]

Now K_{eq} (in eq 2), the true thermodynamic binding constant, is obtained by extrapolating the log K_b plot to $I^{1/2} = 0$. Since the effect of ionic strength is absent here, the magnitude of K_{eq} should depend solely upon the charge interactions between the ligand and the receptor pocket. The calculated value of K_{eq} (Table 2) at the respective pH for the HSA–CR, HSA–TZ, and HSA–WF cases is found to decrease significantly between pH 4.8 and 7.3. Interestingly, for CM and C314, we do not see any such change in K_{eq} with pH. Thus, the pH-dependent behavior of receptor–ligand interaction, if any, can also be followed from the variation of K_{eq}.

Except for CM and C314, the absolute value of the product $Z_D \cdot Z_P$ is found to change considerably on moving from pH 4.8 to pH 7.3 (Table 2). In the studied pH range, CR and TZ are tri-negative, CM is di-negative, WF is mono-negative, and C314 is a neutral species.[54] Taking Z_D values as mentioned, we have calculated Z_P, the average positive charge experienced by the ligand in the receptor pocket (Table 3) at different pH. Importantly, Z_P is also found to be affected by pH, except for CM and C314. The data indicates that Z_P at a given pH is neither constant nor the same for different ligands carrying the same amount of charge (like CR and TZ). Rather, the receptor pocket effective charge depends on the ligand itself and the charge on the ligand does not appear to be the sole determining factor. Also, the difference of Z_P (i.e., $\Delta Z_P = Z_{P,pH4.8} - Z_{P,pH7.3}$) on switching from pH 4.8 to 7.3 comes out to be 0.8 for HSA–CR and 1.7 for HSA–TZ (Table 3). For warfarin, we get $\Delta Z_P = 0.7$ taking $Z_D = -1$, and for CM, $\Delta Z_P \sim 0$ for $Z_D = -2$ (between pH 5.6 and 7.3). Actually, ΔZ_P is a measure of the possible number of charge unit alterations in the receptor pocket due to change of pH.

The surroundings within 15 Å radii around Trp214 of HSA have been examined (figure not shown) using Visual Molecular

Table 3. Effect of pH on the Magnitude of Z_P for HSA–Ligand Systems[a]

			Z_P				
Z_D	ligand	protein	pH 4.8	pH 5.6	pH 6.4	pH 7.3	$\Delta Z_P = Z_{P,pH4.8} - Z_{P,pH7.3}$
−3	CR	HSA	2.6 ± 0.02	2.6 ± 0.03	1.8 ± 0.01	1.8 ± 0.02	0.8 ± 0.1
−3	TZ	HSA	3.2 ± 0.03	2.8 ± 0.02	1.5 ± 0.04	1.5 ± 0.05	1.7 ± 0.15
−2	CM	HSA	1.7 ± 0.01	1.9 ± 0.01	1.7 ± 0.01	1.7 ± 0.02	∼0
−1	WF	HSA	NA	2.1 ± 0.02	1.1 ± 0.02	1.4 ± 0.06	0.7 ± 0.1
0	C314	HSA	NA	NA	NA	NA	NA

[a]NA = not attempted.

dx.doi.org/10.1021/jp407057f | J. Phys. Chem. B 2014, 118, 26–36

Dynamics software (VMD 1.8.7).[69] The fluorophore (Trp214) in HSA is found to be surrounded by positively charged side chains of histidine (His, pK_a = 6.1), lysine (Lys, pK_a = 10.4), and arginine (Arg, pK_a = 12). At pH 4.8 (pI of HSA), when the overall charge of protein is neutral, the electrostatic interaction (attraction) between those positively charged amino acid side chains (His, Lys, and Arg) in the anion receptor pocket and negatively charged ligand (negative sulfonate groups/any other negative group) results in high binding, as expected. When the pH of the medium increases, some of these side chains (e.g., His) may get deprotonated to the solvent. This reduces the net local positive charge, so the ion-pair formation (electrostatic binding) between the ligand and the receptor pocket becomes weak. Thus, the receptor pocket effective charge gets modulated with pH.

It will be interesting to explore when a neutral ligand binds to site-I of HSA. In this regard, we have used one site-I binder neutral ligand C314 and studied the effect of ionic strength on its binding (Table 2). As expected, in this case, ionic strength dependency of the binding constant is not observed (Figure 2) and also the product $Z_D Z_P \sim 0$. This again confirms the applicability of eq 2 that, for (+·0) interaction, the strength of binding should not change with ionic strength; hence, the case of C314 binding can be regarded as non-electrostatic. Thus, the external factors like pH and ionic strength do not seem to be important in the receptor−ligand system when the interaction is not guided by electrostatic forces.

We could not find any suitable positively charged ligands which bind to subdomain IIA of HSA with a high affinity; this is probably because binding of cationic ligand in the anion receptor pocket, as expected, will be weak.

Besides the experimental studies described above, molecular docking explorations provide useful details of the preferred binding location and orientation of the ligand.

3.3. Energy Transfer between Tryptophan and Ligands (TZ and C314). Assuming that quenching of HSA fluorescence is solely due to energy transfer between donor (the tryptophan residue) and acceptor (ligands), we can estimate the distance between them by applying Förster nonradiative energy transfer theory.[70] Since among all the ligands the absorption spectra of only TZ and C314 have greater overlap with the emission spectra of HSA, these are considered as acceptors for the calculation. This theory relates the energy transfer efficiency (E) to the distance between the donor (r) and the acceptor molecule and also calculates the critical distance (R_0).

$$E = 1 - \frac{F}{F^0} = \frac{{R_0}^6}{{R_0}^6 + r^6} \tag{3}$$

$${R_0}^6 = 8.8 \times 10^{-25} \kappa^2 N^{-4} \varphi J \tag{4}$$

where κ^2 is the spatial orientation factor. N is the refractive index of the medium. φ is the fluorescence quantum yield of the donor in the absence of acceptor. J is the spectral overlap integral of the donor fluorescence emission spectrum and the acceptor absorption spectrum, and it is given by

$$J = \frac{\sum F(\lambda)\varepsilon(\lambda)\lambda^4 \Delta\lambda}{\sum F(\lambda)\Delta\lambda} \tag{5}$$

where $F(\lambda)$ is the fluorescence intensity of donor at wavelength λ and $\varepsilon(\lambda)$ is the molar absorption coefficient of acceptor at wavelength λ. The values of E, J, R_0, and r are calculated assuming $\kappa^2 = 2/3$, $N = 1.4$, and $\varphi = 0.15$[38] at all the studied pH values and also in the presence of added salt concentrations (0.05 and 0.2 M NaCl) and listed in Table 4.

Table 4. Energy Transfer Distances between Donor (Tryptophan) and Ligands (TZ and C314) at Different pH and Added Salt Concentration at 298 K

	energy transfer distance (r in nm)		
system	0.0 M NaCl	0.05 M NaCl	0.2 M NaCl
	HSA−TZ		
pH 4.8	2.10 ± 0.07	2.48 ± 0.05	3.36 ± 0.06
pH 5.6	2.34 ± 0.09	2.77 ± 0.03	3.65 ± 0.07
pH 6.4	2.38 ± 0.05	2.82 ± 0.08	3.48 ± 0.06
pH 7.3	2.43 ± 0.04	2.84 ± 0.03	3.34 ± 0.08
	HSA−C314		
pH 5.6	2.85 ± 0.09	2.86 ± 0.10	2.87 ± 0.08
pH 6.4	2.86 ± 0.05	2.87 ± 0.05	2.87 ± 0.06
pH 7.3	2.85 ± 0.04	2.86 ± 0.10	2.87 ± 0.07

From Table 4, it is observed that the distance between the tryptophan residue and TZ is increased with an increase of pH, indicating weaker interaction and hence lower rate of energy transfer, whereas the distance between tryptophan and C314 remains almost unaffected with change of pH. The values of R_0 and r at different pH are lower than the maximal critical distance for R_0 (5−10 nm) and the maximum critical distance between donor and acceptor for r (7−10 nm),[38] which indicates the possibility of efficient energy transfer from HSA to ligands (TZ and C314).

Table 4 also shows that the r value gets progressively increased with increasing salt concentration for the HSA−TZ system, whereas for the HSA−C314 system it remains almost unaffected with added electrolyte concentration. These results also indicate that TZ binds with HSA electrostatically, whereas C314 binds non-electrostatically. Moreover, it is important to note that the distance between the tryptophan and ligand is significantly altered (by ∼1.2 units) when salt concentration is varied compared to that in pH variation (by ∼0.4 units).

Now as mentioned earlier (in the section 1) that charge residing on a side chain at some distant region from the binding pocket of HSA may vary with pH, which could, in principle, alter the strength of electrostatic interaction between protein and ligand. However, the energy transfer calculation shows that the distance between tryptophan 214 and ligand is not very significantly affected by pH compared to the case of salt addition. In the latter case, a substantial increase in energy transfer distance is observed. The added salt weakens the strength of specific electrostatic binding of ligand in the protein pocket, and hence, the distances between the tryptophan residue and ligand increase. Therefore, the role of pocket charges seems more important than the overall/surface charge of the macromolecule in the pocket-specific electrostatic interaction of the studied ligands.

3.4. Docking Studies for Different Ligands and Crystal Structure Data for Warfarin−HSA Complex. In this article, we also investigate the docking of cochineal red A, tartrazine, carmoisine, and C314 into the 3D structure of HSA to account for the experimental findings. Crystal structure data for HSA-WF[56] is also discussed. If we combine the results obtained from our experiments and docking simulations, we have the following points to make:

dx.doi.org/10.1021/jp407057f | J. Phys. Chem. B 2014, 118, 26−36

(a) All ligands bind in subdomain IIA, i.e., site-I near Trp214 of HSA. The distances between ligands and Trp214 are found within 5.5−7.0 Å (see Table S1 in the Supporting Information). The distance between warfarin and Trp214 is found to be 12.7 Å from the crystal structure. Considerable loss of accessible surface area (ASA) of Trp214 is observed upon docking of the ligand (see Tables S2, S3, S4, S5, and S6 in the Supporting Information).

(b) The number of binding sites (n) of CR/TZ/CM at pH 4.8 for HSA (Table 2) is found to be a little higher than unity. The loss of solvent accessible area (ΔASA) of Pro447, Cys448, Asp451, and Tyr452, the residues located at the interface of subdomains IIA and IIIA, shows some distinct changes in the concerned subdomain (see Tables S2, S3, and S4 in the Supporting Information). A common interface between subdomains IIA and IIIA, stabilized by both hydrophobic and salt bridge interactions,[71] is also found from the crystal structure of HSA. Thus, the single tryptophan in HSA that is monitored in the binding study participates in an additional hydrophobic packing interaction of the IIA−IIIA interface.[72] Thus, any perturbation near Trp214 in subdomain IIA may induce changes in subdomain IIIA as well. For the secondary effect, just discussed, the value of n tends to become a little more than unity. The binding site number (n) may also become a bit higher than unity due to the stronger binding interaction in the anion receptor pocket at pH 4.8.

(c) A closer look into the (ligand) binding site of CR (Figure 3), TZ, and WF (see Figures S6a and S7a in the Supporting Information) reveals that the positively charged amino acid residues, such as Lys, Arg, and His, are in close vicinity of docked ligands and the electrostatic interaction between those amino acid side chains with anionic ligands is an obvious consequence. Loss of ASA of these positive amino acid residues also supports their (electrostatic) interaction with negative ligand in the anion receptor pocket (Tables S2, S3, and S5 in the Supporting Information). Importantly, all three ligands, CR, TZ, and WF, show the pH sensitive binding between pH 4.8 and 7.3 (Table 2), and the corresponding ΔZ_P values for these ligands are $\Delta Z_{P,CR} \sim 1$, $\Delta Z_{P,TZ} \sim 2$, and $\Delta Z_{P,WF} \sim 1$, respectively. This change in Z_P can be brought about by the alteration of the side chain charge of some amino acid residues in the anion receptor pocket. Interestingly, the analysis of the lowest energy docked pose of CR, TZ and the crystal structure of HSA−WF indicate availability of nearby (within ∼3 Å) His residue(s) in the ligand binding site. Deprotonation of this (these) histidine side chain(s) due to increase of pH above its pK_a value ($pK_{a,His} = 6.1$) may explain the calculated ΔZ_P values (see Table S7 in the Supporting Information).

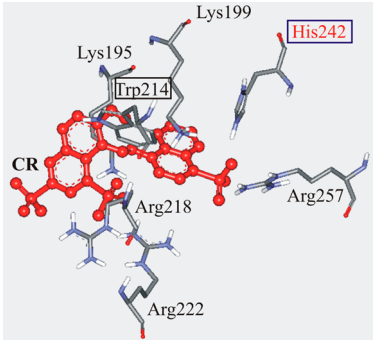

Figure 3. Interacting amino acid residues around the binding site of docked cochineal red A (CR) in subdomain IIA of HSA.

(d) Despite being a negative dye ligand, the binding of CM is found to be pH-insensitive between 4.8 and 7.3 (Table 2) and the corresponding $\Delta Z_P = 0$. However, the loss of ASA of Arg218 and Arg222 indicates electrostatic interaction with the positive side chains (see Table S4 in the Supporting Information). Possibly CM finds a place in the receptor pocket different from that of CR or TZ. Molecular docking also shows that CM does not have a nearby (within ∼3 Å, available with other ligands) histidine side chain (Figure S6b in the Supporting Information). The distance between His 242 and CM is found to be 6.1 Å, which is at much larger separation and may not have any effect (see Table S1 in the Supporting Information). Thus, pH sensitivity of ligand binding in the pH range 4.8−7.3, for CR, TZ, can result from the charge alteration of the receptor pocket due to protonation or deprotonation of the positively charged amino acid side chain (possibly His). The ionizable amino acid side chain in the receptor pocket, other than that of His, Lys, and Arg residues, could be an aspartate (Asp 451) with $pK_a \sim 4$.[73] The docked poses indicate Asp 451 is at relatively large separations (∼7.3−8.7 Å) from the ligand, and hence less likely to contribute to the pocket charge alterations due to pH.

(e) For HSA−C314, the docking analysis indicates that the histidine side chain is within 6.4 Å and there are nearby Lys195, Lys199, Arg218, 222, and 257 side chains in site-I (see Table S6 and Figure S7b in the Supporting Information). However, since C314 is a neutral ligand, its binding in the receptor pocket will not be via electrostatic interaction. Thus, the binding constant remains unchanged with pH.

Therefore, molecular docking studies have been found to corroborate the conclusions from the experimental results complemented by the Debye−Hückel theory.

4. CONCLUSION

The exploration of pH- and ionic-strength-dependent interaction of several site-I specific anionic ligands with HSA clearly reveals that subdomain IIA is primarily an anion receptor pocket. On applying the Debye−Hückel limiting law to the data at different ionic strengths, we have observed a nice linear correlation of the logarithm of the binding constant with the square root of ionic strength. The applicability of the limiting law indicates that the point-charge approximation is valid in such cases where the interaction takes place in a very small part of the protein (receptor pocket). The novelties of the present approach are (1) we can find out the nature of charge interactions, i.e., whether it is the same type or opposite charge-type interaction (electrostatic) or charged−uncharged (non-electrostatic) case, (2) the local charge of the receptor pocket has been found to be more important in such interactions than the overall charge of the biomolecule, and (3) we can find out the effective electrostatic charge of the receptor pocket as experienced by the ligand. This receptor effective charge is also characteristic of the ligand used. (4) Another important insight about such protein based receptor pocket is that it does not always make use of the same amount of charge to stabilize the interaction, and (5) the true thermodynamic binding constant (K_{eq}) can be found out.

Our data also shows that the binding constant depends very much on the ionic strengths of the medium. Thus, ideally, any report of electrostatic binding should refer to the ionic strength

dx.doi.org/10.1021/jp407057f | J. Phys. Chem. B 2014, 118, 26−36

used. On the other hand, the use of K_{eq} does not require the ionic strength reference and hence its use is more convenient here than K_b.

Proteins are large macromolecules having many conformations and distributed charges, and on the other hand, Debye–Hückel limiting law ignores the finite size of the interacting ions. Apparently, it looks like that these two aspects may not go side by side. However, our experimental data at different ionic strengths are found to nicely corroborate the Debye–Hückel prescriptions. Since binding is confined in a smaller region (receptor pocket) of protein, local electrostatic interaction is more important so that the large protein size can be neglected. The generality of the present study shows that the technique can be applied to *any* receptor–ligand electrostatic interaction to explore the nature of the host.

The present study indicates that, when the interaction between protein (receptor) and ligand is dominated by electrostatic forces, external factors like pH and ionic strength are very crucial in determining the strength of interaction. Proper optimization of these two factors with respect to any receptor–ligand pair can indeed render the drug effective.

■ ASSOCIATED CONTENT

Supporting Information

Figure S1: Effect of selected site markers on HSA–coumarin 314 in 5 mM phosphate buffer of pH 7.3 and 298 K. [HSA] = 2 μM and [protein]:[site marker] = 1:1. Symbols with cap include error bar. Figure S2: Quenching plot of HSA–cochineal red A in the presence of an increasing concentration of NaCl at pH 7.3 (red color) and 4.8 (black color) and 298 K. Symbols with cap include error bar. Figure S3: Quenching plot of the HSA–tartrazine system in the presence of increasing concentrations of NaCl at pH 4.8 and 298 K. (●) 0 M, (▲) 0.05 M, and (■) 0.2 M NaCl. Symbols with cap include error bar. Figure S4: Quenching plot of the HSA–carmoisine and HSA–coumarin 314 systems in the presence of (●) 0 M, (▲) 0.05 M, and (■) 0.2 M NaCl at pH 7.3 and 298 K. Symbols with cap include error bar. Figure S5: Job's plot of HSA–coumarin 314 systems at pH 7.3 and 298 K. Symbols with cap include error bar. Figure S6: Interacting amino acid residues around the binding site of (a) tartrazine and (b) carmoisine in subdomain IIA. Figure S7: Interacting amino acid residues around the binding site of (a) warfarin and (b) coumarin 314 in subdomain IIA of HSA. Table S1: Distances (in Å) between the amino acid residues in the binding site of HSA with ligands. Table S2: Change in accessible surface area (ΔASA) in Å^2 of interacting residues of HSA (uncomplexed) and their complex with cochineal red A. Table S3: Change in accessible surface area (ΔASA) in Å^2 of interacting residues of HSA (uncomplexed) and their complex with tartrazine. Table S4: Change in accessible surface area (ΔASA) in Å^2 of interacting residues of HSA (uncomplexed) and their complex with carmoisine. Table S5: Change in accessible surface area (ΔASA) in Å^2 of interacting residues of HSA (uncomplexed) and their complex with warfarin. Table S6: Change in accessible surface area (ΔASA) in Å^2 of interacting residues of HSA (uncomplexed) and their complex with coumarin 314. Table S7: Comparison of the number of histidine residues in the receptor pocket of HSA with ΔZ_p values for different ligands. This material is available free of charge via the Internet at http://pubs.acs.org.

■ AUTHOR INFORMATION

Corresponding Author

*Phone: +91-3222-283314. Fax: +91-3222-282252. E-mail: mintu@chem.iitkgp.ernet.in.

Notes

The authors declare no competing financial interest.

■ ACKNOWLEDGMENTS

We thank DST-India, CSIR-India, and IIT-Kharagpur for financial support. P.B. thanks CSIR-India for an individual research associateship. S.D. thanks IIT-Kharagpur for an institutional fellowship. N.M. thanks CSIR-India for providing an individual fellowship. We would like to thank the anonymous reviewers for their critical comments and suggestions.

■ REFERENCES

(1) Allard, J. F.; Dushek, O.; Coombs, D.; van der Merwe, P. A. Mechanical Modulation of Receptor-Ligand Interactions at Cell-Cell Interfaces. *Biophys. J.* **2012**, *102*, 1265–1273.

(2) Rich, R. L.; Hoth, L. R.; Geoghegan, K. F.; Brown, T. A.; LeMotte, P. K.; Simons, S. P.; Hensley, P.; Myszka, D. G. Kinetic Analysis of Estrogen Receptor/ Ligand Interactions. *Proc. Natl. Acad. Sci. U.S.A.* **2002**, *99*, 8562–8567.

(3) Ballardini, R.; Balzani, V.; Credi, A.; Gandolfi, M. T.; Hibert, F. K.; Lehn, J. M.; Prodi, L. Supramolecular Photochemistry and Photophysics. A Cylindrical Macrotricyclic Receptor and Its Adducts with Protons, Ammonium Ions, and a Pt (II) Complex. *J. Am. Chem. Soc.* **1994**, *116*, 5741–5746.

(4) Agasti, S. S.; Liong, M.; Tassa, C.; Chung, H. J.; Shaw, S. Y.; Lee, H.; Weissleder, R. Supramolecular Host–Guest Interaction for Labeling and Detection of Cellular Biomarkers. *Angew. Chem., Int. Ed.* **2012**, *51*, 450–454.

(5) Gellman, S. H. Introduction: Molecular Recognition. *Chem. Rev.* **1997**, *97*, 1231–1232.

(6) Berde, C. B.; Hudson, B. S.; Simon, R. D.; Sklar, L. A. Human Serum Albumin. Spectroscopic Studies of Binding and Proximity Relationships for Fatty Acids and Bilirubin. *J. Biol. Chem.* **1979**, *254*, 391–400.

(7) Schneider, H.-J.; Yatsimirsky, A. K. Selectivity in Supramolecular Host–Guest Complexes. *Chem. Soc. Rev.* **2008**, *37*, 263–277.

(8) Pal, B.; Bajpai, P. K.; Baul, T. S. B. Binding of 5-(2 '-Carboxyphenyl)Azoquinolin-8-Ol to Bovine Serum Albumin: A Spectroscopic Study. *Spectrochim. Acta, Part A* **2000**, *56*, 2453–2458.

(9) Lyon, C. E.; Suh, E. S.; Dobson, C. M.; Hore, P. J. Probing the Exposure of Tyrosine and Tryptophan Residues in Partially Folded Proteins and Folding Intermediates by Cidnp Pulse-Labeling. *J. Am. Chem. Soc.* **2002**, *124*, 13018–13024.

(10) Cheng, L. T.; Wang, Z.; Setny, P.; Dzubiella, J.; Li, B.; McCammon, J. A. Interfaces and Hydrophobic Interactions in Receptor-Ligand Systems: A Level-Set Variational Implicit Solvent Approach. *J. Chem. Phys.* **2009**, *131*, 144102–144111.

(11) Ma, M.; Paredes, A.; Bong, D. Intra- and Intermembrane Pairwise Molecular Recognition between Synthetic Hydrogen Bonding Phospholipids. *J. Am. Chem. Soc.* **2008**, *130*, 14456–14458.

(12) Bader, A. N.; Van Dongen, M. M.; Van Lipzig, M. M. H.; Kool, J.; Meerman, J. H. N.; Ariese, F.; Gooijer, C. The Chemical Interaction between the Estrogen Receptor and Monohydroxybenzo[a]Pyrene Derivatives Studied by Fluorescence Line-Narrowing Spectroscopy. *Chem. Res. Toxicol.* **2005**, *18*, 1405–1412.

(13) Colquhoun, H. M.; Zhu, Z.; Williams, D. J. Extreme Complementarity in a Macrocycle Tweezer Complex. *Org. Lett.* **2003**, *5*, 4353–4356.

(14) Branco, T. J. F.; Vieira Ferreira, L. F.; Botelho do Rego, A. M.; Oliveira, A. S.; Da Silva, J. P. Pyrene–P-Tert-Butylcalixarenes Inclusion Complexes Formation: A Surface Photochemistry Study. *Photochem. Photobiol. Sci.* **2006**, *5*, 1068–1077.

(15) Baudry, R.; Kalchenko, O.; Dumazet-Bonnamour, I.; Vocanson, F.; Lamartine, R. Investigation of Host−Guest Stability Constants of Calix[n]Arenes Complexes with Aromatic Molecules by RP-HPLC Method. *J. Chromatogr. Sci.* **2003**, *41*, 157−163.
(16) Kakuta, T.; Takashima, Y.; Harada, A. Highly Elastic Supramolecular Hydrogels Using Host−Guest Inclusion Complexes with Cyclodextrins. *Macromolecules* **2013**, *46*, 4575−4579.
(17) Baudoin, O.; Gonnet, F.; Teulade-Fichou, M. P.; Vigneron, J. P.; Tabet, J. C.; Lehn, J. M. Molecular Recognition of Nucleotide Pairs by a Cyclo-Bis-Intercaland-Type Receptor Molecule: A Spectrophotometric and Electrospray Mass Spectrometry Study. *Chem.—Eur. J.* **1999**, *5*, 2762−2771.
(18) Kukić, P.; Nielsen, J. E. Electrostatics in Proteins and Protein−Ligand Complexes. *Future Med. Chem.* **2010**, *2*, 647−666.
(19) Jakoby, M. G.; Miller, K. R.; Toner, J. J.; Bauman, A.; Cheng, L.; Li, E.; Cistola, D. P. Ligand Protein Electrostatic Interactions Govern the Specificity of Retinol-Binding and Fatty Acid-Binding Proteins. *Biochemistry* **1993**, *32*, 872−878.
(20) Linderstrøm-Lang, K. On the Ionization of Proteins. *C. R. Trav. Lab. Carlsberg* **1924**, *15*, 1−29.
(21) Shishkov, I. F.; Khristenko, L. V.; Rudakov, F. M.; Vilkov, L. V.; Karlov, S. S.; Zaitseva, G. S.; Samdal, S. The Molecular Structure of Boratrane Determined by Gas Electron Diffraction and Quantum Mechanical Calculations. *J. Mol. Struct.* **2002**, *641*, 199−205.
(22) Bhattacharya, B.; Nakka, S.; Guruprasad, L.; Samanta, A. Interaction of Bovine Serum Albumin with Dipolar Molecules: Fluorescence and Molecular Docking Studies. *J. Phys. Chem. B* **2009**, *113*, 2143−2150.
(23) Jang, H.; Hall, C. K.; Zhou, Y. Q. Protein Folding Pathways and Kinetics: Molecular Dynamics Simulations of Beta-Strand Motifs. *Biophys. J.* **2002**, *83*, 819−835.
(24) de Oliveira, C. A. F.; Guimaraes, C. R. W.; Barreiro, G.; de Alencastro, R. B. Investigation of the Induced-Fit Mechanism and Catalytic Activity of the Human Cytomegalovirus Protease Homodimer Via Molecular Dynamics Simulations. *Proteins: Struct., Funct., Genet.* **2003**, *52*, 483−491.
(25) Patel, A. B.; Srivastava, S.; Phadke, R. S. Interaction of 7-Hydroxy-8-(Phenylazo) 1,3-Naphthalenedisulfonate with Bovine Plasma Albumin - Spectroscopic Studies. *J. Biol. Chem.* **1999**, *274*, 21755−21762.
(26) Sereikaite, J.; Bumelis, V. A. Interaction of Serum Albumin with Vinyl Sulfonate Azo Dye. *Cent. Eur. J. Chem.* **2008**, *6*, 509−512.
(27) Hutchison, C. A.; Phillips, S.; Edgell, M. H.; Gillam, S.; Jahnke, P.; Smith, M. Mutagenesis at a Specific Position in a DNA-Sequence. *J. Biol. Chem.* **1978**, *253*, 6551−6560.
(28) Thomas, P. G.; Russell, A. J.; Fersht, A. R. Tailoring the pH-Dependence of Enzyme Catalysis Using Protein Engineering. *Nature* **1985**, *318*, 375−376.
(29) Frisch, C.; Schreiber, G.; Johnson, C. M.; Fersht, A. R. Thermodynamics of the Interaction of Barnase and Barstar: Changes in Free Energy Versus Changes in Enthalpy on Mutation. *J. Mol. Biol.* **1997**, *267*, 696−706.
(30) Shang, L.; Jiang, X. U.; Dong, S. J. In Vitro Study on the Binding of Neutral Red to Bovine Serum Albumin by Molecular Spectroscopy. *J. Photochem. Photobiol., A* **2006**, *184*, 93−97.
(31) Otzen, D. E. Protein Unfolding in Detergents: Effect of Micelle Structure, Ionic Strength, pH and Temperature. *Biophys. J.* **2002**, *83*, 2219−2230.
(32) Liang, J. G.; Cheng, Y. P.; Han, H. Y. Study on the Interaction between Bovine Serum Albumin and Cdte Quantum Dots with Spectroscopic Techniques. *J. Mol. Struct.* **2008**, *892*, 116−120.
(33) Park, C.; Raines, R. T. Quantitative Analysis of the Effect of Salt Concentration on Enzymatic Catalysis. *J. Am. Chem. Soc.* **2001**, *123*, 11472−11479.
(34) Szklarczyk, O.; Zuberek, J.; Antosiewicz, J. M. Poisson-Boltzmann Model Analysis of Binding mRNA Cap Analogues to the Translation Initiation Factor Eif4e. *Biophys. Chem.* **2009**, *140*, 16−23.
(35) Mudasir; Wijaya, K.; Wahyuni, E. T.; Yoshioka, N.; Inoue, H. Salt-Dependent Binding of Iron(II) Mixed-Ligand Complexes Containing 1,10-Phenanthroline and Dipyrido[3,2-A: 2 ′,3 ′-C] Phenazine to Calf Thymus DNA. *Biophys. Chem.* **2006**, *121*, 44−50.
(36) Harris, R. C.; Bredenberg, J. H.; Silalahi, A. R. J.; Boschitsch, A. H.; Fenley, M. O. Understanding the Physical Basis of the Salt Dependence of the Electrostatic Binding Free Energy of Mutated Charged Ligand-Nucleic Acid Complexes. *Biophys. Chem.* **2011**, *156*, 79−87.
(37) Zhang, Y. Z.; Zhou, B.; Zhang, X. P.; Huang, P.; Li, C. H.; Liu, Y. Interaction of Malachite Green with Bovine Serum Albumin: Determination of the Binding Mechanism and Binding Site by Spectroscopic Methods. *J. Hazard. Mater.* **2009**, *163*, 1345−1352.
(38) Bolel, P.; Mahapatra, N.; Halder, M. Optical Spectroscopic Exploration of Binding of Cochineal Red A with Two Homologous Serum Albumins. *J. Agric. Food Chem.* **2012**, *60*, 3727−3734.
(39) Datta, S.; Mahapatra, N.; Halder, M. pH-Insensitive Electrostatic Interaction of Carmoisine with Two Serum Proteins: A Possible Caution on Its Uses in Food and Pharmaceutical Industry. *J. Photochem. Photobiol., B* **2013**, *124*, 50−62.
(40) Bolel, P.; Datta, S.; Mahapatra, N.; Halder, M. *J. Phys. Chem. B* **2012**, *116*, 10195−10204.
(41) Izatt, R. M.; Pawlak, K.; Bradshaw, J. S. Thermodynamic and Kinetic Data for Macrocycle Interaction with Cations, Anions, and Neutral Molecules. *Chem. Rev.* **1995**, *95*, 2529−2586.
(42) Roosen-Runge, F.; Heck, B. S.; Zhang, F. J.; Kohlbacher, O.; Schreiber, F. Interplay of pH and Binding of Multivalent Metal Ions: Charge Inversion and Reentrant Condensation in Protein Solutions. *J. Phys. Chem. B* **2013**, *117*, 5777−5787.
(43) Debye, P.; Hückel, E. The Theory of Electrolytes.1.Lowering of Freezing Point and Rleated Phenomena. *Phys. Z.* **1923**, *24*, 185−206.
(44) Debye, P.; Pauling, L. The Inter-Ionic Attraction Theory of Ionized Solutes. Iv. The Influence of Variation of Dielectric Constant on the Limiting Law for Small Concentrations. *J. Am. Chem. Soc.* **1925**, *47*, 2129−2134.
(45) Kragh-Hansen, U. Molecular Aspects of Ligand-Binding to Serum-Albumin. *Pharmacol. Rev.* **1981**, *33*, 17−53.
(46) Lin, J. H.; Cocchetto, D. M.; Duggan, D. E. Protein Binding as a Primary Determinant of the Clinical Pharmacokinetic Properties of Nonsteroidal Antiinflammatory. Drugs. *Clin. Pharmacokinet.* **1987**, *12*, 402−432.
(47) Evans, A. M. Influence of Dietary Components on the Gastrointestinal Metabolism and Transport of Drugs. *Ther. Drug Monit.* **2000**, *22*, 131−136.
(48) Subramanyam, R.; Gollapudi, A.; Bonigala, P.; Chinnaboina, M.; Amooru, D. G. Betulinic Acid Binding to Human Serum Albumin: A Study of Protein Conformation and Binding Affinity. *J. Photochem. Photobiol., B* **2009**, *94*, 8−12.
(49) Rahman, M. H.; Maruyama, T.; Okada, T.; Yamasaki, K.; Otagiri, M. Study of Interaction of Carprofen and Its Enantiomers with Human Serum-Albumin 0.1. Mechanism of Binding Studied by Dialysis and Spectroscopic Methods. *Biochem. Pharmacol.* **1993**, *46*, 1721−1731.
(50) Noonan, J. E.; Meggos, H. Synthetic Food Colours. In *Handbook of Food Additives*, 2nd ed.; Furia, T. E., Ed.; CRC Press: Boca Raton, FL, 1980; pp 339−383.
(51) Wagner, B. D. The Use of Coumarins as Environmentally-Sensitive Fluorescent Probes of Heterogeneous Inclusion Systems. *Molecules* **2009**, *14*, 210−237.
(52) Landefeld, C. S.; Beyth, R. J. Anticoagulant-Related Bleeding - Clinical Epidemiology, Prediction, and Prevention. *Am. J. Med.* **1993**, *95*, 315−328.
(53) Foster, J. F. Some Aspects of the Structure and Conformational Properties of Serum Albumin. In *Albumin Structure, Function and Uses*; Rosenoer, V. M., Oratz, M., Rothschild, M. A., Eds.; Pergamon Press: New York, 1977; pp 53−84.
(54) Minioti, K. S.; Sakellariou, C. F.; Thomaidis, N. S. Determination of 13 Synthetic Food Colorants in Water-Soluble Foods by Reversed-Phase High-Performance Liquid Chromatography Coupled with Diode-Array Detector. *Anal. Chim. Acta* **2007**, *583*, 103−110.

(55) Larsen, F. G.; Larsen, C. G.; Jakobsen, P.; Brodersen, R. Interaction of Warfarin with Human-Serum Albumin - a Stoichiometric Description. *Mol. Pharmacol.* **1985**, *27*, 263−270.
(56) Ghuman, J.; Zunszain, P. A.; Petitpas, I.; Bhattacharya, A. A.; Otagiri, M.; Curry, S. Structural Basis of the Drug-Binding Specificity of Human Serum Albumin. *J. Mol. Biol.* **2005**, *353*, 38−52.
(57) Borissevitch, I. E. More About the Inner Filter Effect: Corrections of Stern-Volmer Fluorescence Quenching Constants Are Necessary at Very Low Optical Absorption of the Quencher. *J. Lumin.* **1999**, *81*, 219−224.
(58) Feng, X. Z.; Lin, Z.; Yang, L. J.; Wang, C.; Bai, C. L. Investigation of the Interaction between Acridine Orange and Bovine Serum Albumin. *Talanta* **1998**, *47*, 1223−1229.
(59) Maes, V.; Engelborghs, Y.; Hoebeke, J.; Maras, Y.; Vercruysse, A. Fluorimetric Analysis of the Binding of Warfarin to Human-Serum Albumin- Equilibrium and Kinetic-Study. *Mol. Pharmacol.* **1982**, *21*, 100−107.
(60) Stewart, J. J. P. *Mopac2009*; Stewart Computational Chemistry: Colorado Springs, CO, 2008.
(61) Morris, G. M.; Goodsell, D. S.; Halliday, R. S.; Huey, R.; Hart, W. E.; Belew, R. K.; Olson, A. J. Automated Docking Using a Lamarckian Genetic Algorithm and an Empirical Binding Free Energy Function. *J. Comput. Chem.* **1998**, *19*, 1639−1662.
(62) *Accelrys Discovery Studio Visualiser V 2.5.1.1967*; Accelrys Software Inc.: San Diego, CA, 2007.
(63) Shahir, A. A.; Javadian, S.; Razavizadeh, B. B. M.; Gharibi, H. Comprehensive. Study of Tartrazine/Cationic Surfactant Interaction. *J. Phys. Chem. B* **2011**, *115*, 14435−14444.
(64) Forte-Tavcer, P. Interactions between Some Anionic Dyes and Cationic Surfactants with Different Alkyl Chain Length Studied by the Method of Continuous Variations. *Dyes Pigm.* **2004**, *63*, 181−189.
(65) Petitpas, I.; Bhattacharya, A. A.; Twine, S.; East, M.; Curry, S. Crystal Structure Analysis of Warfarin Binding to Human Serum Albumin - Anatomy of Drug Site I. *J. Biol. Chem.* **2001**, *276*, 22804−22809.
(66) Atkins, P.; Paula, J. D. *Atkins' Physical Chemistry*, 7th ed.; Oxford University Press Inc.: New York, 2002.
(67) Vlasova, I. M.; Saletsky, A. M. Study of the Denaturation of Human Serum Albumin by Sodium Dodecyl Sulfate Using the Intrinsic Fluorescence of Albumin. *J. Appl. Spectrosc.* **2009**, *76*, 536−541.
(68) Rios, M. A. D.; Plaxco, K. W. Apparent Debye-Huckel Electrostatic Effects in the Folding of a Simple, Single Domain Protein. *Biochemistry* **2005**, *44*, 1243−1250.
(69) Humphrey, W.; Dalke, A.; Schulten, K. VMD: Visual Molecular Dynamics. *J. Mol. Graphics* **1996**, *14*, 33−38.
(70) Lakowicz, J. R. *Principles of Fluorescence Spectroscopy*, 3rd ed.; Springer: New York, 2006.
(71) Carter, D. C.; Ho, J. X. Structure of Serum-Albumin. *Adv. Protein Chem.* **1994**, *45*, 153−203.
(72) Peters, T. J. Serum Albumin. *Adv. Protein Chem.* **1985**, *37*, 161−245.
(73) Khandogin, J.; Brooks, C. L. Toward the Accurate First-Principles Prediction of Ionization Equilibria in Proteins. *Biochemistry* **2006**, *45*, 9363−9373.